JOURNAL OF GEOPHYSICAL RESEARCH, VOL. 102, NO. A7, PAGES 14,149–14,154, JULY 1, 1997

Direct influence of ring current on auroral oval diameter

Michael Schulz
Space Physics Laboratory, Advanced Technology Center, Lockheed Martin Missiles & Space, Palo Alto, California

Abstract. The inside diameter of the auroral oval (conceived as marking the boundary between closed and polar cap field lines) is known to vary with storm intensity, as measured by the *Dst* index. Part of this variability may result from storm-associated changes in solar wind pressure and/or from storm-associated changes in location of the nightside neutral line (inner edge of neutral sheet). The magnetospheric **B** field is also directly distorted (stretched outward) by the stormtime ring current so as to increase the amount of polar cap magnetic flux. The magnitude of this last effect on auroral oval diameter is estimated from a simple model in the present work for storms of various intensities. The prototype for an empty magnetosphere in this effort is Dungey's model (dipole plus uniform southward $B_z \approx -9.0 \cos^6\Lambda^*$ μT, with Λ^* being the invariant latitude of the quiettime auroral oval). Addition of a ring current field $\Delta B_z(r_0)$ with $Dst < 0$ moves the circular neutral line outward (to a larger radial distance r_0 in the equatorial plane) but simultaneously increases the amount of polar cap magnetic flux. The consequent increase in auroral oval diameter can be calculated (in closed form for sufficiently simple ΔB_z models) by magnetic flux bookkeeping. In the present model, this increase ($\equiv -2\,\Delta\Lambda^*$) is typically about 4° ± 1° for each −100 nT of *Dst*.

1. Background

The inside diameter of the auroral oval, conceived [e.g., *Akasofu*, 1977, pp. 13–21; *Feldstein and Galperin*, 1985] as marking the boundary between closed and polar cap field lines becomes enlarged under conditions associated with geomagnetic storms (as indicated by the presence of a strong ring current). Part of this enlargement may be attributed to storm-associated increases in tail field, IMF B_z, or solar wind pressure, but at least part of the remainder must be viewed as a consequence of the ring current itself [cf. *Feldstein*, 1969, p. 194]. The present calculation is intended to illustrate how (and to estimate by how much) the ring current can "stretch field lines open" and thus enlarge the polar cap area enclosed by the auroral oval.

The baseline for the present study is the field model sketched by *Dungey* [1961] but investigated in greater detail by *Hill and Rassbach* [1975]. It consists of a dipole field plus a uniform southward field, such that

$$\mathbf{B} = \mu_E \nabla\,[(1/r^2)\cos\theta - (r/b^3)\cos\theta]\,, \tag{1}$$

where μ_E is the geomagnetic dipole moment, r is the radial distance from the point dipole, θ is the colatitude measured from the dipole axis, and b is the radius of the circular neutral line that marks the boundary between closed and polar cap field lines in this simple axisymmetric model. The equation of a field line in this (baseline) model is

$$r = La\,[1 + \tfrac{1}{2}(r/b)^3]\sin^2\theta\,, \tag{2}$$

where a is the planetary radius and $1/L$ is the limiting value of $(a/r)\sin^2\theta$ as $r \to 0$ along the field line. The value of L corresponding to the last closed field line (called L^*) is thus $2b/3a$, and so (for example) the polar cap boundary resides at "invariant" magnetic latitude $\Lambda = \Lambda^* = 70°$ (colatitude $\theta^* = 20°$) if $L^* = 8.547$ ($b = 12.8205a$). The uniform southward field $\hat{\mathbf{z}}\mu_E(a/b)^3$ in this case amounts to −14.332 nT for $\mu_E = 0.302$ G-R_E^3 [*IAGA Division 5, Working Group 8*, 1996]. It corresponds (topologically and otherwise) to the tail field [*Schulz*, 1976, 1991, pp. 106, 108–109] and not to the interplanetary magnetic field (IMF).

Paper number 97JA00827.
0148-0227/97/97JA-00827$09.00

2. Ring Current Field Model

The present study requires (of course) a model for the magnetic field produced by the ring current. This model need not be global, however. An expression for the radial dependence of the equatorial field perturbation ΔB_z (parallel to the dipole axis) turns out to be sufficient. The model used here for the equatorial ΔB_z produced by the ring current is illustrated in Figure 1. It corresponds to the functional representation

$$\Delta B_{rc} = B_{01}, \quad 0 \le r \le r_1 \tag{3a}$$

$$\Delta B_{rc} = B_{01} + [(r-r_1)/(r_2-r_1)](B_{23}-B_{01})\,, \quad r_1 \le r \le r_2 \tag{3b}$$

$$\Delta B_{rc} = B_{23}\,, \quad r_2 \le r \le r_3 \tag{3c}$$

$$\Delta B_{rc} = B_{23} + [(r-r_3)/(r_4-r_3)](B_4-B_{23})\,, \quad r_3 \le r \le r_4 \tag{3d}$$

$$\Delta B_{rc} = -0.4(r_5/r^2)^3(r^3 - r_5^3)B_{23}\,, \quad r \ge r_4 \tag{3e}$$

with adjustable parameters $r_1 = 2.00R_E$, $r_2 = 3.59R_E$, $r_3 = 4.00R_E$, $r_4 = 4.986118279R_E$, and $r_5 = 5.70R_E$; also $B_{23} = 1.6B_{01}$ and $B_4 = 0.472282817B_{01}$. (Values quoted to unusual precision belong to derived parameters; see below.) The model field perturbation ΔB_z varies piecewise linearly with r except at $r > r_4$, and the smooth curve in this outermost region represents a field that becomes dipolar asymptotically.

The parameter B_{01} (< 0) in (3) corresponds to a locally uniform southward magnetic field perturbation in the region immediately surrounding the Earth. The values of r_4 and B_4 are determined by requiring that (3d) join smoothly with (3e) at $r = r_4$. The maximum positive ΔB_{rc} (attained at $r = 2^{1/3}r_5$) is made equal to −0.16 B_{01} in this model. Other parameter assignments in (3) are based

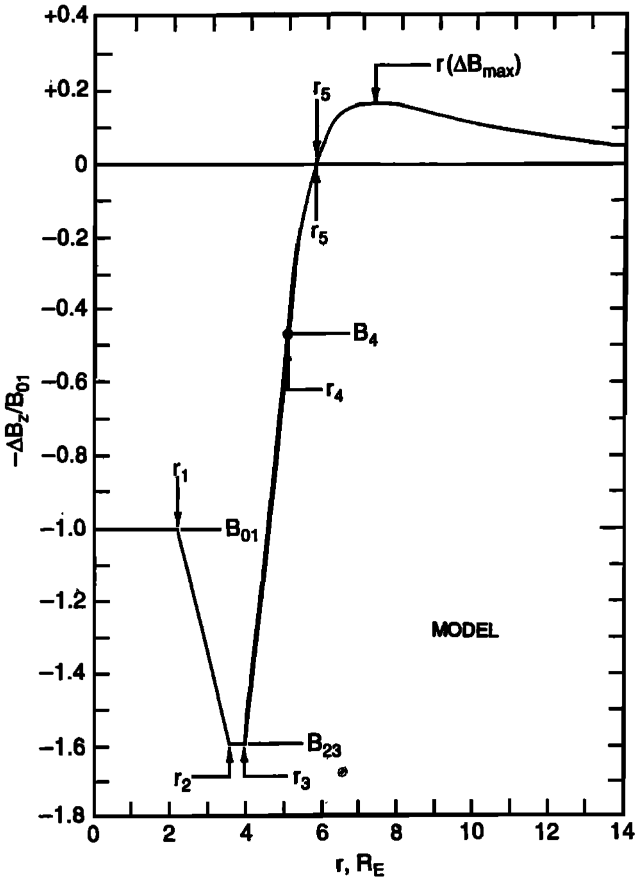

Figure 1. Ring current field model defined by (3). Radii r_n (n = 1–5) and field strengths (B_{01}, B_{23}, B_4) are scalable (but not independently adjustable) parameters of the model (constrained by piecewise linearity of ΔB_{rc} with r for $r \le r_4$, smooth continuity of ΔB_{rc} at $r = r_4$, and magnetic flux conservation).

on visual impressions of various ring current field models [e.g., *Hoffman and Bracken*, 1967, p. 6043; *Søraas and Davis*, 1968, p. 28; *Chen et al.*, 1994, p. 5753] and adjusted as necessary so as to conserve magnetic flux. (The positive flux at $r > r_5$ balances the negative flux at $r < r_5$ to about one part in 10^7 in this example.) The model ring current field in Figure 1 scales in field intensity with B_{01} and can be scaled radially by applying a common factor to all the $\{r_n\}$ for n = 1–5. Results based on simulations of the particle transport needed to produce the stormtime ring current [*Chen et al.*, 1994] suggest that values assigned to the $\{r_n\}$ should perhaps vary inversely with $|Dst|$, but this refinement is left out of the present work.

From the equatorial field model specified by (3), it is easy to calculate the amount of magnetic flux outside any magnetic shell of equatorial radius r. The partial result needed for use in the present study is

$$\Phi_{rc} = -1.28\pi r_5^2 (r_5/r)[1-\tfrac{1}{4}(r_5/r)^3]B_{01}, \quad r \ge r_4 \qquad (4)$$

In particular, the amount of positive magnetic flux Φ_{rc} at $r > r_5$ is equal to $-0.96\pi r_5{}^2 B_{01}$, and the amount of negative flux Φ_{rc} at $r < r_5$ is equal to $+0.96\pi r_5{}^2 B_{01}$.

3. Earth Induction

The magnetic field generated by the ring current is approximately uniform, not only at the equator for $r < r_1 \approx 2\ R_E$, but throughout a spherical volume of this radius surrounding the Earth [e.g., *Hoffman and Bracken*, 1965]. Under the approximation that this magnetic field is excluded from penetrating a sphere of radius $r_c \le a$ inside the Earth, the ring current can be considered to "induce" a dipole of moment $(r_c{}^3/2)B_{01}$, which is generated by an azimuthal current (in a direction opposite to the ring current) on the surface of the sphere at $r = r_c$. It proves convenient to introduce a shielding parameter $\varepsilon \equiv (r_c/a)^3$, such that the stormtime B_{01} fully penetrates the Earth for $\varepsilon = 0$ but is totally excluded from the Earth (i.e., totally draped around it) for $\varepsilon = 1$. Calculations by *McDonald* [1957] suggest that $\varepsilon \sim 0.7$–0.8 at frequencies (~ 5–25 μHz) of interest in the present context [*Søraas and Davis*, 1968, p. 31].

The induced-dipole (id) field is perpendicular to the equatorial plane, where its strength is given by $\Delta B_{id} = -B_{01}$ for $0 \le r < r_c$ and by

$$\Delta B_{id} = (r_c^3/2r^3)B_{01} = \varepsilon(a^3/2r^3)B_{01} \qquad (5)$$

for $r > r_c$. The induced dipole thus accounts for up to 30% of the equatorial ΔB_z observed at $r = a$ and commonly identified with Dst. The other 70% (at least) of Dst must then come from (3a) in the absence of other contributions to equatorial ΔB_z. For completeness, however, the model should include the possibility of a uniform stormtime increase ΔB_t (< 0) in the tail field, which might be added to $-(\mu_E/b^3)$ in (1) and thus to B_{01} in (5). Any such ΔB_t would contribute to the observed Dst and would thus relieve the trapped (ring current) particle population from part of this burden [e.g., *Campbell*, 1996].

4. Magnetic Flux Bookkeeping

The foregoing considerations suggest a model magnetic field perpendicular to the equatorial plane and given by

$$B_z = (\mu_E/r^3) - (\mu_E/b^3) + \Delta B_{rc} + \Delta B_t + \varepsilon(B_{01} + \Delta B_t)(a^3/2r^3) \qquad (6)$$

there (i.e., at z = 0). With the help of (3), this expression for equatorial B_z applies from $r = r_c$ to the radius of the neutral line. The radius b^* (> r_4) of the neutral line is found by solving (6) for $B_z = 0$, using (3e) to represent ΔB_{rc} for $r > r_4$. Because of the convenient form of (3e), this amounts to solving a quadratic equation for $(r/b)^3$. While the term ΔB_t constitutes somewhat of a "wild card" in (6), only two test cases are contemplated in the present study: The first calls for $\Delta B_t \equiv 0$, while the second calls for ΔB_t to assume whatever value would make b^* equal to the original b (= 12.8205a), so as to maintain the same neutral line radius as before the storm.

The eventual goal here is to map the neutral line (which marks the boundary between closed and polar cap field lines) to the planetary surface ($r = a$). This mapping must follow a magnetic shell, for which no form can be specified explicitly in the absence of a global model for **B**. The mapping strategy thus contemplates an axisymmetric Gaussian surface that consists of a planar annulus extending from the planetary surface ($r = a$) to the neutral line ($r = b^*$) in the equatorial (z = 0) plane, the northern half of the magnetic shell that marks the boundary between closed and polar cap field lines, and a zone extending from the boundary between closed and polar cap field lines ($\theta = \theta^*$) to the equator ($\theta = \pi/2$) on the planetary surface ($r = a$). The concept is illustrated in Figure 2, which uses as its template the baseline field model specified by (1).

The amount of magnetic flux crossing the Gaussian surface described above can be expressed as follows:

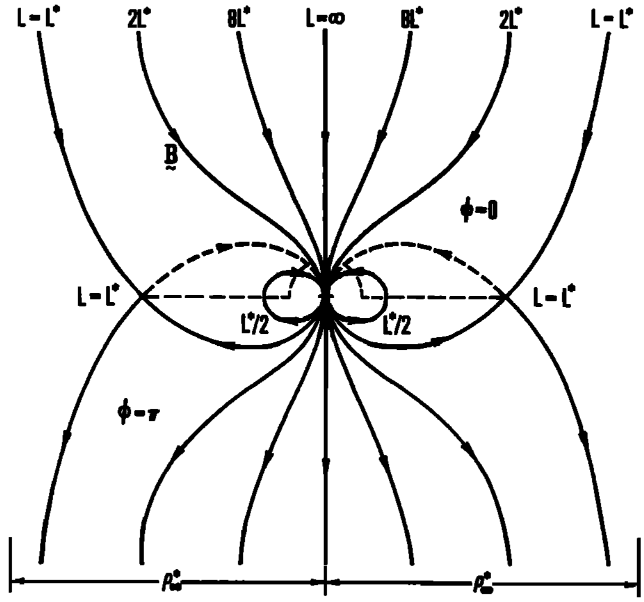

Figure 2. Illustration of Gaussian surface (dashed curve) used for mapping neutral line to Earth's surface (enlarged for clarity) by invoking magnetic flux conservation in the present model. Field model is that inspired by *Dungey* [1961] and obtained by adding uniform southward "tail" field B_t [*Schulz*, 1976] to dipolar magnetic field [see also *Hill and Rassbach*, 1975]. Closed field lines have $L < L^*$; polar cap field lines have $L > L^*$.

$$2\pi \int_{a\ [z=0]}^{b^*} r\, B_z\, dr \; + \; 2\pi \int_{0\ [r=a]}^{\cos\theta^*} r^2\, B_r\, d(\cos\theta) \; = \; 0 \qquad (7)$$

In other words, the amount of magnetic flux crossing the equatorial ($z = 0$) plane between $r = a$ and the radius of the neutral line ($r = b^*$) must balance the amount of magnetic flux crossing the planetary surface between $\theta = \theta^*$ and the equator ($\theta = \pi/2$). After all, no magnetic flux can cross a magnetic shell that is aligned with **B** by construction, even if there is no algorithm for the construction.

Evaluation of the second integral in (7) requires an expression for the radial component of **B** at $r = a$, namely

$$B_r \; = \; [-\,2(\mu_E/a^3) \; - \; (\mu_E/b^3) \; + \; (1-\varepsilon)(B_{01} + \Delta B_t)]\cos\theta\,. \qquad (8)$$

This last expression follows from (6), in the sense that the three terms proportional to $1/r^3$ there correspond to dipolar **B** fields, whereas the three constant terms in (6) correspond to fields that are uniform at least for $r \lesssim r_1$. The second term in (7) is thus equal to

$$2\pi \int_{0\ [r=a]}^{\cos\theta^*} r^2\, B_r\, d(\cos\theta) \; = \; -\,\pi a^2\,[2(\mu_E/a^3) \; + \; (\mu_E/b^3) \; - \; (1-\varepsilon)(B_{01} + \Delta B_t)]\cos^2\theta^*\,, \qquad (9a)$$

and the amount of polar cap magnetic flux is equal to

$$2\pi \int_{\cos\theta^*\ [r=a]}^{1} r^2\, B_r\, d(\cos\theta) \; = \; -\,\pi a^2\,[2(\mu_E/a^3) \; + \; (\mu_E/b^3) \; - \; (1-\varepsilon)(B_{01} + \Delta B_t)]\sin^2\theta^*\,. \qquad (9b)$$

This last result will be useful (see below) for estimating the asymptotic stormtime radius ρ_∞^* of the magnetotail, corresponding to the bundle of polar cap field lines in Figure 2.

Evaluation of the first integral in (7) is straightforward, except that the contribution from the term ΔB_{rc} in (6) is easier to calculate indirectly via (4) than directly via (3): Since (3) has already been shown to conserve magnetic flux, it follows that

$$2\pi \int_{a\ [z=0]}^{b^*} r\, \Delta B_{rc}\, dr \; = \; -\,2\pi \int_{0\ [z=0]}^{a} r\, \Delta B_{rc}\, dr \; - \; 2\pi \int_{b^*\ [z=0]}^{\infty} r\, \Delta B_{rc}\, dr$$
$$= \; -\,\pi a^2 B_{01} \; + \; 1.28\pi r_5^2 (r_5/b^*)[1 - \tfrac{1}{4}(r_5/b^*)^3] B_{01}\,, \qquad (10a)$$

whereupon

$$2\pi \int_{a\ [z=0]}^{b^*} r\, B_z\, dr \; = \; \pi\{2(\mu_E/a) - 2(\mu_E/b^*) + [\Delta B_t - (\mu_E/b^3)]\,[(b^*)^2 \; - \; a^2] - a^2 B_{01} + 1.28 r_5^2 (r_5/b^*)[1 - \tfrac{1}{4}(r_5/b^*)^3] B_{01} + \varepsilon(B_{01} + \Delta B_t)\, a^2\,[1 - (a/b^*)]\}. \qquad (10b)$$

Substitution of (9a) and (10b) in (7) conveniently yields

$$\pi a^2\,[2(\mu_E/a^3) \; + \; (\mu_E/b^3) \; - \; (1-\varepsilon)(B_{01} + \Delta B_t)]\sin^2\theta^*$$
$$= \; \pi\{2(\mu_E/b^*) \; + \; [(\mu_E/b^3) \; - \; \Delta B_t](b^*)^2 \; + \; \varepsilon(B_{01} + \Delta B_t)(a^3/b^*) \; - \; 1.28 r_5^2 (r_5/b^*)[1 - \tfrac{1}{4}(r_5/b^*)^3] B_{01}\} \qquad (11)$$

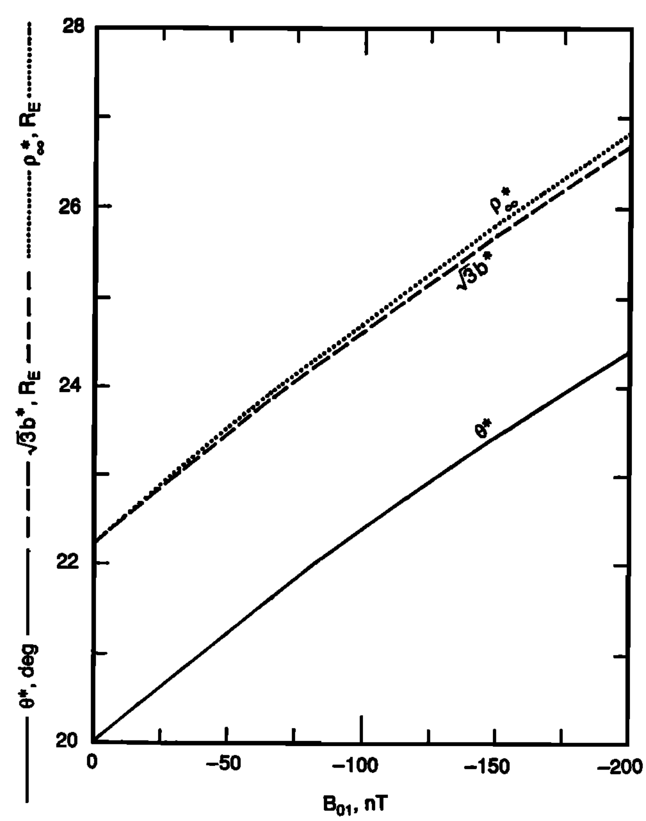

Figure 3. Results for auroral oval radius (magnetic colatitude) θ^*, asymptotic tail radius ρ_∞^*, and radius b^* of neutral line (multiplied by $\sqrt{3}$ for comparison with ρ_∞^*), plotted as functions of model parameter B_{01} (ring current field at $0 \le r \le r_1$) for $\Delta B_t = 0$ (tail field held constant).

after some cancellation of terms facilitated by setting $\cos^2\theta^* = 1 - \sin^2\theta^*$. This last result is simultaneously an equation for $\sin^2\theta^*$ (= $\cos^2\Lambda^*$) and also an expression comparable to (9b) for the amount of polar cap magnetic flux. In other words, the right-hand side of (11) must equal $\pi(\rho_\infty{}^*)^2[(\mu_E/b^3) - \Delta B_t]$, where $\rho_\infty{}^*$ is the asymptotic radius of the "magnetotail" in Figure 2 as $|z| \to \infty$. Recovered from (11) is the familiar result [e.g., *Hill and Rassbach*, 1975] that $\rho_\infty{}^* = \sqrt{3}b^* = \sqrt{3}b$ for $B_{01} = \Delta B_t = 0$, which corresponds to the baseline model specified by (1).

5. Numerical Results

Algebraic results obtained above express the magnetic colatitude (θ^*) of the auroral oval, the radius (b^*) of the neutral line, and the asymptotic radius ($\rho_\infty{}^*$) of the "magnetotail" in terms of the stormtime augmentation ΔB_t of the tail field and the near-Earth strength (B_{01}) of the magnetic field produced by the ring current. This last quantity is proportional in first approximation [*Dessler and Parker*, 1959; *Sckopke*, 1966] to the total energy content of the trapped-particle population. The value of *Dst* in the present model would be equal to $[1 + (\varepsilon/2)](B_{01} + \Delta B_t)$, including the effect of Earth induction.

Since the purpose of the present work is to illustrate how the ring current itself can "stretch field lines open" so as to enlarge the auroral oval, the first numerical example treated here is for $\Delta B_t = 0$. The results for θ^*, $\sqrt{3}b^*$, and $\rho_\infty{}^*$ are plotted in Figure 3 as functions of $|B_{01}|$. The results for $\varepsilon = 0$ (no Earth induction) and $\varepsilon = 1$ (full Earth induction) are visually indistinguishable from each other in Figure 3, and it is safe to assume that a realistic value for ε (~ 0.7–0.8) would yield an intermediate result for each of the parameters thus calculated (θ^*, $\sqrt{3}b^*$, $\rho_\infty{}^*$). (The purpose in plotting $\sqrt{3}b^*$ rather than b^* is to show how nearly invariant the ratio $\sqrt{3}b^*/\rho_\infty{}^*$ remains as B_{01} is allowed to vary.) The boundary between closed and polar cap field lines in Figure 3 seems to move about 2.3° equatorward for each 100 nT of B_{01}, presumably corresponding to about 140 nT of *Dst*.

The neutral line radius b^* in Figure 3 increases with the strength of the storm, as measured by $|B_{01}|$. This trend (which may seem unrealistic) just reflects the fact that the magnetic moment of the ring current augments the magnetic moment of the Earth. What may be unrealistic about Figure 3 is the assumption that $\Delta B_t = 0$. Accordingly, for the second numerical example treated here, it is assumed that ΔB_t varies with B_{01} so as to maintain $b^* = b$. The results for θ^*, $\sqrt{3}b^*$, and $\rho_\infty{}^*$ are plotted in Figure 4 as functions of $B_{01} + \Delta B_t$. The rationale for choosing $B_{01} + \Delta B_t$ as abscissa is its direct observability, magnified by the Earth-induction factor $1 + (\varepsilon/2)$, in the form of *Dst*. It follows from (3e) and (6) that the corresponding variation of ΔB_t with B_{01} is given by

$$\frac{\Delta B_t}{B_{01}} = \frac{0.64(r_5/b)^3[1-(r_5/b)^3]-(\varepsilon/2)(a/b)^3}{1+(\varepsilon/2)(a/b)^3} = \begin{cases} 0.05130, & \varepsilon = 0 \\ 0.05105, & \varepsilon = 1 \end{cases} \qquad (12)$$

in this scenario ($b^* = b$). The results for $\varepsilon = 0$ (no Earth induction) and $\varepsilon = 1$ (full Earth induction) are again visually indistinguishable from each other, and it is safe to assume that a realistic value for ε (~ 0.7–0.8) would yield an intermediate result for each of the parameters thus calculated (Λ^*, $\sqrt{3}b^*$, $\rho_\infty{}^*$; ΔB_t). In Figure 4 the boundary between closed and polar cap field lines seems to move about 3.2° equatorward for each 100 nT of $B_{01} + \Delta B_t$, presumably corresponding to about 140 nT of *Dst*. It might be more realistic to postulate a $|\Delta B_t|$ large enough to reduce the stormtime neutral line radius b^* to values less than the quiettime value (b). This would let the time-varying tail field contribute more significantly to *Dst*, as *Campbell* [1996] has suggested it should, and would lead as well to a more pronounced increase in auroral oval diameter with increasing $|Dst|$.

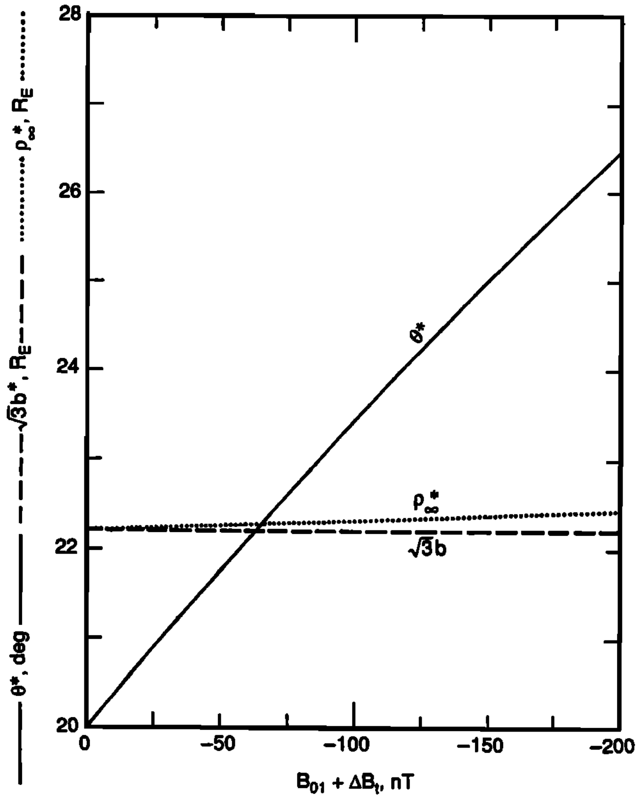

Figure 4. Results for auroral oval radius (magnetic colatitude) θ^* and asymptotic tail radius $\rho_\infty{}^*$, plotted as functions of $B_{01} + \Delta B_t$ (to which *Dst* should be proportional in this model) for $b^* = b$ (tail field increased by $\Delta B_t \approx 0.051 B_{01}$ so as to keep radius of neutral line constant). Horizontal line representing constant $\sqrt{3}b^* = \sqrt{3}b$ is shown for comparison with $\rho_\infty{}^*$.

After having completed the present study, the author learned of a philosophically similar calculation by *Akasofu* [1963], who considered the outward "stretching" of field lines by a model ring current and invoked magnetic flux conservation to estimate the resulting outward displacements of equatorial crossing points in an image-dipole model of the magnetosphere. This was before *Ness* [1965] had discovered the geomagnetic tail, and so *Akasofu* [1963] did not seek to distinguish between closed and polar cap field lines as such. He did, however, clearly associate deformation of magnetic shells by the ring current (and changes in their equatorial intercepts relative to the boundary of the magnetosphere) with changes in the position of the auroral oval. The present model does provide a somewhat improved treatment of the problem, in that here the auroral oval is associated with an analytically calculated boundary between closed and polar cap field lines. However, *Akasofu* [1963] had clearly anticipated the physical effect investigated here and had similarly exploited magnetic flux conservation to estimate its magnitude.

6. Comparison With Observational Data

The solid curves in Figures 3 and 4 suggest an increase of $5.5° \mp 0.9°$, respectively, in auroral oval diameter for each 100 nT change in $B_{01} + \Delta B_t$. Since these results pertain to an axisymmetric field model, they should be compared with observational data on a global parameter, preferably the inside diameter of the auroral oval, rather than with data on the latitude of the aurora at any particular magnetic local time (MLT). Thus, for example, a comparison with the stormtime oval diameters deduced from the DMSP data of *Meng* [1984] would be appropriate.

In Figures 1 and 3 of *Meng* [1984], the distance from the middle of the cusp to the poleward boundary of the nightside auroral oval appears to have been about 30° under pre-storm conditions and about 50° when *Dst* reached its most negative value (−156 nT and −120 nT, respectively, for the two storms considered). These *Dst* values would correspond to $B_{01} + \Delta B_z$ = −110 nT and −85 nT, respectively, in the present work. This would suggest an increase of 18.2° to 23.5° per 100 nT of $B_{01} + \Delta B_z$.

Earlier data of *Akasofu and Chapman* [1963, Figure 4] from ground-based auroral observations taken during the International Geophysical Year (IGY, 1957–1958) suggest a 3.5° equatorward displacement of quiet arcs on the nightside auroral oval for each 100 nT of $B_{01} + \Delta B_z$. This would be an encouraging result, except that the latitude of the auroral oval shows much more dayside variability than nightside variability [e.g., *Feldstein*, 1969]. In other words, the center of the auroral oval is offset from the magnetic pole by an amount that varies inversely with the inside diameter of the oval, which is in fact almost circular [*Meng et al.*, 1977].

In a more exhaustive study *Meng and Makita* [1986] have examined the variation of auroral oval diameter with various other indices such as *AE* and IMF B_z, which also exert a strong influence on the oval. As has been noted in section 1 (the introduction), various physical processes might influence the size of the stormtime oval. The purpose of this work has been to estimate how large an influence the ring current itself might have. This is mostly a theoretical question, since other magnetospheric parameters that should likewise influence auroral oval diameter tend to be positively correlated with *Dst*.

7. Further Discussion

Akasofu et al. [1961, p. 4025] pointed out that the ring current itself generates a magnetic moment which augments Earth's magnetic moment as presented to the solar wind. The present model ring current yields, according to (3e), a magnetic moment $\mu_{rc} = -0.64 r_5^3 B_{01}$ parallel to the Earth's dipole moment ($\mu_E = 0.302$ G-R_E^3). The two moments would be equal (thus doubling the effective moment presented to the solar wind) for $B_{01} \approx -254$ nT ($Dst \approx -356$ nT), which can be attained in a very major storm. The radii $\{r_n\}$ in (3) are held constant (independent of B_{01}) in the calculations underlying Figures 3 and 4, but (as has been noted above) the model ring-current field in Figure 1 would remain flux-conserving if all the $\{r_n\}$ were multiplied by a common scaling factor, which might vary inversely with B_{01}.

Kuznetsov [1996] has recently proposed model in which the magnetic moment of the stormtime ring current essentially independent of *Dst*. This would correspond to a scaling of all the $\{r_n\}$ in the present model by a factor inversely proportional to the cube root of $|B_{01}|$. By making the leading terms in (3e) and (4) independent of B_{01}, it would also eliminate any significant variation of θ^* with *Dst* in Figures 3 and 4. Such a model would thus defeat the purpose of the present work. It can be shown, in fact, that the total magnetic moment produced (through gyration and drift) by a specified population of geomagnetically trapped particles would remain invariant under radial diffusion that conserves the first two adiabatic invariants of charged-particle motion while violating the third invariant.

The simulation results of *Chen et al.* [1994] suggest a more weakly inverse variation of the $\{r_n\}$ with $|B_{01}|$, which would preserve the sense of the present results but reduce the magnitude that could be claimed for the direct effect a stormtime ring current on the diameter of the auroral oval and geomagnetic tail. How can these results be reconciled with invariance of the total magnetic moment under radial diffusion? Most of the stormtime increase in magnetospheric particle energy content found in the simulations of *Chen et al.* [1994] can be attributed to particles which were not originally trapped, but which became trapped after having been introduced across the neutral line during the course of the simulated storm. The stormtime ring current thus does not constitute "a specified population" in the sense needed to make its total magnetic moment invariant under radial diffusion.

8. Summary

The present calculation has fulfilled its goal of illustrating how (and of estimating by how much) the ring current can "stretch field lines open" so as to enlarge the polar cap area enclosed by the auroral oval. It could be used in this context as a classroom example or homework exercise. Obviously, however, the real magnetosphere is more complicated than the simple model developed here. Truly quantitative estimates of ring current effects on auroral oval position and diameter require the numerical analysis of a more realistic model for the magnetosphere. *Stern* [1985] has noted in this context that the place to which the polar cleft region (associated with dayside neutral points on the magnetopause) maps on the Earth's surface should be displaced equatorward by up to 2° for each change of −100 nT in the parameter corresponding to B_{01}. The present results suggest that mappings of the nightside neutral line are affected by at least a similar amount.

Acknowledgments. This work (insofar as it pertains to the aurora) has been supported in part by NASA contract NAS5-30372 for PIXIE (the X-ray imager on the GGS/POLAR satellite), in part by NSF grant ATM-9119516 for interpretation of Søndre Strømfjord radar data, and in part by the Independent Research and Development (IRAD) program of Lockheed Martin Missiles & Space. The previously unpublished analytical ring current model specified by (3) had already been developed with support from the U.S. Air Force Phillips Laboratory under contract F19628-90-C-0097 for the interpretation of energetic particle data from the CRRES satellite. The author also thanks R. A. Hoffman for helpful clarifications of his previous work on ring current modeling. Both referees have been helpful, and one of them in particular directed the author's attention to important work on this subject in the existing literature.

The Editor thanks S.-I. Akasofu and the other referee for their assistance in evaluating this paper.

References

Akasofu, S.-I., Deformation of magnetic shells during magnetic storms, *J. Geophys. Res.*, *68*, 4437–4445, 1963.

Akasofu, S.-I., *Physics of Magnetospheric Substorms*, D. Reidel, Norwell, Mass., 1977.

Akasofu, S. I., and S. Chapman, The lower limit of latitude (US sector) of northern quiet auroral arcs, and its relation to *Dst(H)*, *J. Atmos. Terr. Phys.*, *25*, 9–12, 1963.

Akasofu, S.-I., J. C. Cain, and S. Chapman, The magnetic field of a model radiation belt, numerically computed, *J. Geophys. Res.*, *66*, 4013–4026, 1961.

Campbell, W. H., Geomagnetic storms, the *Dst* ring-current myth and lognormal distributions, *J. Atmos. Terr. Phys.*, *58*, 1171–1187, 1996.

Chen, M. W., L. R. Lyons, and M. Schulz, Simulations of phase space distributions of storm time proton ring current, *J. Geophys. Res.*, *99*, 5745–5759, 1994.

Dessler, A. J., and E. N. Parker, Hydromagnetic theory of geomagnetic storms, *J. Geophys. Res.*, *64*, 2239–2252, 1959.

Dungey, J. W., Interplanetary magnetic field and the auroral zones, *Phys. Rev. Lett.*, *6*, 47–48, 1961.

Feldstein, Y. I., Polar auroras, polar substorms, and their relationships with the dynamics of the magnetosphere, *Rev. Geophys.*, *7*, 179–218, 1969.

Feldstein, Y. I., and Yu. I. Galperin, The auroral luminosity structure in the high-latitude upper atmosphere: Its dynamics and relationship to the large-scale structure of the Earth's magnetosphere, *Rev. Geophys.*, *23*, 217–275, 1985.

Hill, T. W., and M. E. Rassbach, Interplanetary magnetic field direction and the configuration of the day side magnetosphere, *J. Geophys. Res.*, *80*, 1–6, 1975.

Hoffman, R. A., and P. A. Bracken, Magnetic effects of the quiet-time proton belt, *J. Geophys. Res.*, *70*, 3541–3556, 1965.

Hoffman, R. A., and P. A. Bracken, Higher-order ring currents and particle energy storage in the magnetosphere, *J. Geophys. Res.*, *72*, 6039–6049, 1967.

IAGA Division V, Working Group 8, Revision of International Geomagnetic Reference Field released, *Eos Trans. AGU*, *77*, 153, 1996.

Kuznetsov, S. N., A model of ring current based on the Dessler-Parker-Sckopke theorem, *Radiat. Meas.*, *26*, 400–404, 1996.

McDonald, K. L., Penetration of the geomagnetic secular variation through a mantle with variable conductivity, *J. Geophys. Res.*, *62*, 117–141, 1957.

Meng, C.-I., Dynamic variation of the auroral oval during intense magnetic storms, *J. Geophys. Res.*, *89*, 227–235, 1984.

Meng, C.-I., and K. Makita, Dynamic variations of the polar cap, in *Solar Wind-Magnetosphere Coupling*, edited by Y. Kamide and J. A. Slavin, pp. 605–631, Terra Scientific, Tokyo, 1986.

Meng, C.-I., R. H. Holzworth, and S.-I. Akasofu, Auroral circle—Delineating the poleward boundary of the quiet auroral belt, *J. Geophys. Res.*, *82*, 164–172, 1977.

Ness, N. F., The Earth's magnetic tail, *J. Geophys. Res.*, *70*, 2989–3005, 1965.

Schulz, M., Plasma boundaries in space, in *Physics of Solar Planetary Environments*, edited by D. J. Williams, vol. 1, pp. 491–504, AGU, Washington, D. C., 1976.

Schulz, M., The magnetosphere, in *Geomagnetism*, edited by J. A. Jacobs, vol. 4, pp. 87–293, Academic, San Diego, Calif., 1991.

Schulz, M., and M. C. McNab, Source-surface modeling of planetary magnetospheres, *J. Geophys. Res.*, *101*, 5095–5118, 1996.

Sckopke, N., A general relation between the energy of trapped particles and the disturbance field near the Earth, *J. Geophys. Res.*, *71*, 3125–3130, 1966.

Stern, D. P., Parabolic harmonics in magnetospheric modeling: The main dipole and the ring current, *J. Geophys. Res.*, *90*, 10851–10863, 1985.

Søraas, F., and L. R. Davis, Temporal variations of the 100 keV to 1700 keV trapped protons observed on satellite Explorer 26 during first half of 1965, *Rept. X-612-68-328*, NASA Goddard Space Flight Center, Greenbelt, Md., 1968.

M. Schulz, Space Physics Laboratory, Advanced Technology Center, Lockheed Martin Missiles & Space (O/H1-11, B/252), 3251 Hanover Street, Palo Alto, CA 94304. (e-mail: schulz@agena.space.lockheed. com)

(Received May 10, 1996; revised November 15, 1996; accepted March 5, 1997.)